JOURNAL OF BACTERIOLOGY, July 2004, p. 4705–4713 Vol. 186, No. 14
0021-9193/04/$08.00+0 DOI: 10.1128/JB.186.14.4705–4713.2004

Altering Toluene 4-Monooxygenase by Active-Site Engineering for the Synthesis of 3-Methoxycatechol, Methoxyhydroquinone, and Methylhydroquinone

Ying Tao,[1] Ayelet Fishman,[1] William E. Bentley,[2] and Thomas K. Wood[1]*

Departments of Chemical Engineering and Molecular and Cell Biology, University of Connecticut, Storrs, Connecticut 06269-3222,[1] and Department of Chemical Engineering, University of Maryland, College Park, Maryland 20742[2]

Received 20 February 2004/Accepted 16 April 2004

Wild-type toluene 4-monooxygenase (T4MO) of *Pseudomonas mendocina* KR1 oxidizes toluene to *p*-cresol (96%) and oxidizes benzene sequentially to phenol, to catechol, and to 1,2,3-trihydroxybenzene. In this study T4MO was found to oxidize *o*-cresol to 3-methylcatechol (91%) and methylhydroquinone (9%), to oxidize *m*-cresol and *p*-cresol to 4-methylcatechol (100%), and to oxidize *o*-methoxyphenol to 4-methoxyresorcinol (87%), 3-methoxycatechol (11%), and methoxyhydroquinone (2%). Apparent V_{max} values of 6.6 ± 0.9 to 10.7 ± 0.1 nmol/min/mg of protein were obtained for *o*-, *m*-, and *p*-cresol oxidation by wild-type T4MO, which are comparable to the toluene oxidation rate (15.1 ± 0.8 nmol/min/mg of protein). After these new reactions were discovered, saturation mutagenesis was performed near the diiron catalytic center at positions I100, G103, and A107 of the alpha subunit of the hydroxylase (TmoA) based on directed evolution of the related toluene *o*-monooxygenase of *Burkholderia cepacia* G4 (K. A. Canada, S. Iwashita, H. Shim, and T. K. Wood, J. Bacteriol. *184*:344-349, 2002) and a previously reported T4MO G103L regiospecific mutant (K. H. Mitchell, J. M. Studts, and B. G. Fox, Biochemistry 41:3176-3188, 2002). By using *o*-cresol and *o*-methoxyphenol as model substrates, regiospecific mutants of T4MO were created; for example, TmoA variant G103A/A107S produced 3-methylcatechol (98%) from *o*-cresol twofold faster and produced 3-methoxycatechol (82%) from 1 mM *o*-methoxyphenol seven times faster than the wild-type T4MO (1.5 ± 0.2 versus 0.21 ± 0.01 nmol/min/mg of protein). Variant I100L produced 3-methoxycatechol from *o*-methoxyphenol four times faster than wild-type T4MO, and G103S/A107T produced methylhydroquinone (92%) from *o*-cresol fourfold faster than wild-type T4MO and there was 10 times more in terms of the percentage of the product. Variant G103S produced 40-fold more methoxyhydroquinone from *o*-methoxyphenol than the wild-type enzyme produced (80 versus 2%) and produced methylhydroquinone (80%) from *o*-cresol. Hence, the regiospecific oxidation of *o*-methoxyphenol and *o*-cresol was changed for significant synthesis of 3-methoxycatechol, methoxyhydroquinone, 3-methylcatechol, and methylhydroquinone. The enzyme variants also demonstrated altered monohydroxylation regiospecificity for toluene; for example, G103S/A107G formed 82% *o*-cresol, so saturation mutagenesis converted T4MO into an *ortho*-hydroxylating enzyme. Furthermore, G103S/A107T formed 100% *p*-cresol from toluene; hence, a better *para*-hydroxylating enzyme than wild-type T4MO was formed. Structure homology modeling suggested that hydrogen bonding interactions of the hydroxyl groups of altered residues S103, S107, and T107 influence the regiospecificity of the oxygenase reaction.

Substituted catechols, especially 3-substituted catechols, are useful precursors for making pharmaceuticals (14); one of these compounds, 3-methoxycatechol, is an important intermediate for the antivascular agents combretastatin A-1 and combretastatin B-1 (5). Methoxyhydroquinone is used in the synthesis of triptycene quinones that have been shown to have anti-leukemia cell activity (16), and methylhydroquinone has been recently reported to be used in the synthesis of (±)-helibisabonol A and puraquinonic acid, which are precursors of agrochemical herbicides and antileukemia drugs, respectively (15, 20). Manufacture of these substituted dihydroxylated compounds by chemical routes is difficult due to the employment of aggressive reagents, expensive and complicated starting materials, multiple reaction steps, and low yields (14). Therefore, alternatives to chemical synthesis of these important industrial intermediates have been investigated.

* Corresponding author. Mailing address: Departments of Chemical Engineering and Molecular and Cell Biology, 191 Auditorium Road, U-3222, University of Connecticut, Storrs, CT 06269-3222. Phone: (860) 486-2483. Fax: (860) 486-2959. E-mail: twood@engr.uconn.edu.

Biocatalysis has become an attractive alternative to chemical synthesis because of its high selectivity and efficiency. For example, it can produce relatively pure compounds compared with the racemic mixtures often obtained by chemical methods (6). Biocatalysis also avoids tedious blocking and deblocking steps which are common in the chemical synthesis of enantio- and regioselective compounds (37), and it is inherently environmentally benign as the reactions are usually performed in water (avoiding harsh solvents) at room temperature and atmospheric pressure under milder conditions (1).

Lately, a large number of enzymes have been studied for aromatic hydroxylations, such as heme P450s, flavin monooxygenases, pterin-dependent nonheme monooxygenases, nonheme mononuclear iron dioxygenases, and diiron hydroxylases (24). For example, Meyer et al. (23) reported that directed evolution with error-prone PCR increased the substrate specific activity of the flavoenzyme 2-hydroxybiphenyl 3-monooxygenase twofold towards *o*-methoxyphenol and fivefold towards 2-*tert*-butylphenol for making the corresponding 3-substituted catechols. Canada et al. (6) used DNA shuffling to evolve

toluene *ortho*-monooxygenase (TOM) from *Burkholderia cepacia* G4 for 1-naphthol synthesis, and one mutant (TomA3 V106A) with sixfold-increased activity was found. Furthermore, substituted catechols (e.g., 3-bromocatechol, 3-methoxycatechol, 3-iodocatechol, and 3-methylcatechol) were synthesized from substituted benzenes in two steps by using recombinant *Escherichia coli* expressing both toluene dioxygenase and dihydrocatechol dehydrogenase (5).

Toluene 4-monooxygenase (T4MO) from *Pseudomonas mendocina* KR1 belongs to the family of diiron hydroxylases that includes the methane, toluene, benzene, and *o*-xylene monooxygenases, phenol hydroxylases, and alkene epoxidases (25). T4MO is a soluble, nonheme, O_2-dependent, diiron monooxygenase consisting of a 211-kDa hydroxylase (encoded by *tmoAEB*) with an $(\alpha\beta\gamma)_2$ quaternary structure, a 36-kDa NADH oxidoreductase (encoded by *tmoF*) containing flavin adenine dinucleotide and a [2Fe-2S] cluster, a 12.5-kDa Rieske-type [2Fe-2S] ferredoxin (encoded by *tmoC*) involved in electron transfer between the hydroxylase and the reductase, and a 11.6-kDa protein (encoded by *tmoD*) as a catalytic effector (40). All six genes are required for efficient multiple catalysis and high regiospecificity. The $(\alpha\beta\gamma)_2$ hydroxylase component containing the diiron catalytic center for substrate binding and the hydroxylation reaction (29) was reported recently to be responsible for the monooxygenation regiospecificity of T4MO, while the binding of the effector protein refined the product distribution leading to high regiospecificity (25).

T4MO of *P. mendocina* KR1 is the most efficient toluene-oxidizing enzyme in the toluene monooxygenase family, which includes TOM (26), toluene *para*-monooxygenase (formerly toluene 3-monooxygenase [10]) of *Ralstonia pickettii* PKO1, and toluene/*o*-xylene monooxygenase of *Pseudomonas stutzeri* OX1 (4). T4MO oxidizes toluene to 96% *p*-cresol, 2.8% *m*-cresol, 0.4% *o*-cresol, and 0.8% benzyl alcohol (29). However other enzymes (for example, ammonia monooxygenase, chloroperoxidase, cytochromes P450, methane monooxygenase, and xylene monooxygenase) oxidize alkylbenzenes and produce benzyl alcohols (70 to 100% of the total products) and only negligible amounts of phenolic products (29). The high regiospecificity for *para* hydroxylation of toluene and the nearly nonexistent activity for the methyl group make T4MO a valuable enzyme for aromatic ring hydroxylation. In addition, T4MO has a broad substrate specificity for mono-substituted benzenes, including nitrobenzene, chlorobenzene, and methoxybenzene, which were reported to be catalyzed to single hydroxylated products in the *para* position (29). We discovered recently that T4MO can perform three successive hydroxylations, resulting in conversion of benzene to phenol, catechol, and subsequently 1,2,3-trihydroxybenzene (42). Thus, T4MO is an attractive biocatalyst for performing up to three regiospecific aromatic ring hydroxylations.

Based on the enhanced rate of naphthalene oxidation by TOM TomA3 V106A (6), here we used saturation mutagenesis at the analogous position TmoA I100 of T4MO to explore all the substitutions for this codon. In addition, codon A113 of TOM TomA3 was found to be responsible for the regiospecific hydroxylation of indole (32a); hence, the analogous position, TmoA A107, was also subjected to saturation mutagenesis. Furthermore, based on primary sequence alignments with other toluene, phenol, and alkene monooxygenases, mutagenesis was performed previously by Fox and coworkers on T4MO; T4MO TmoA site-directed mutagenesis G103L, A107G, Q141C, I180F, and F205I variants, as well as saturation mutagenesis T201 mutants, were used to identify amino acid residues contributing to the hydroxylation regiospecificity of toluene (24, 25, 28, 29; B. G. Fox, oral presentation, 102nd Gen. Meet. Am. Soc. Microbiol., 2002). They found that the T4MO TmoA G103L mutant had enhanced *ortho* hydroxylation of toluene (55% *o*-cresol) (24, 25) and that combining this mutation with an A107G mutation resulted in the formation of primarily *o*-cresol from toluene (Fox, Abstr. 102nd Gen. Meet. Am. Soc. Microbiol.), so position G103 of TmoA was also mutated in this study. There have been no previous reports of making functionalized dihydroxylated aromatics with T4MO, as these reactions were not discovered previously (42).

Here, *o*-methoxyphenol and *o*-cresol were chosen as substrates for the engineered T4MO TmoA due to the potential of the oxidation products of these substrates for applications in the synthesis of both pharmaceuticals and industrial chemicals. We report four new products for wild-type T4MO; wild-type T4MO produces 4-methoxyresorcinol as the major product from *o*-methoxyphenol, produces 3-methylcatechol and methylhydroquinone from *o*-cresol, and produces 4-methylcatechol from *m*- and *p*-cresol. Saturation mutagenesis was also used to change the regiospecificity and to expand the product spectrum for three novel, industrially significant products (3-methoxycatechol, methoxyhydroquinone, and methylhydroquinone) and convert T4MO into an *ortho*-hydroxylating enzyme, as well as a better *para*-hydroxylating enzyme.

MATERIALS AND METHODS

Chemicals. *o*-Methoxyphenol (guaiacol), 3-methoxycatechol, and *p*-cresol were obtained from Acros Organics (Morris Plains, N.J.). *o*-Cresol, *m*-cresol, methoxyhydroquinone, 3-methylcatechol, 4-methylcatechol, and methylhydroquinone were obtained from Sigma-Aldrich Co. (Milwaukee, Wis.). 4-Methoxyresorcinol and 2-methoxyresorcinol were obtained from INDUFINE Chemical Co., Inc. (Hillsborough, N.J.). All materials used were of the highest purity available and were used without further purification.

Bacterial strains, plasmids, and growth conditions. Plasmid pBS(Kan)T4MO, which constitutively expresses T4MO *tmoABCDEF*, was constructed as described previously (42). In pBS(Kan)T4MO, the *lac* promoter yields constitutive expression of T4MO due to the high copy number of the plasmid and the lack of the *lacI* repressor. Kanamycin resistance was added to pBS(Kan)T4MO to reduce plasmid segregational instability. *E. coli* TG1 [*supE hsd*Δ5] *thi* Δ(*lac-proAB*) F′ (*traD*36 *proAB*$^+$ *lacI*^{q} *lacZ*ΔM15) expressing wild-type and mutant T4MO from plasmid pBS(Kan)T4MO was used as the whole-cell biocatalyst.

Cells were routinely cultivated at 37°C with shaking at 250 rpm on a C25 incubator shaker (New Brunswick Scientific Co., Edison, N.J.) in Luria-Bertani (LB) medium (35) supplemented with kanamycin (100 μg/ml). Exponential-phase cultures were used in all experiments by inoculating single colonies and growing cultures to an optical density at 600 nm (OD_{600}) of 1.5. Cells were centrifuged at 13,000 × *g* for 5 min at 25°C in a J2-HS centrifuge (Beckman, Palo Alto, Calif.). The collected cells were resuspended in 50 mM Tris-HCl buffer (pH 7.4) or in 50 mM Tris-HNO_3 buffer (pH 7.4).

Protein analysis and molecular techniques. The total protein concentration of TG1/pBS(Kan)T4MO was determined to be 0.24 mg of protein/ml/OD_{600} unit by using a Total Protein kit (Sigma Chemical Co., St. Louis, Mo.) (42). Cellular protein samples were analyzed on sodium dodecyl sulfate—12% polyacrylamide gels and then stained with Coomassie brilliant blue (35). Plasmid DNA was isolated with a Midi or Mini kit (QIAGEN, Inc., Chatsworth, Calif.), and DNA fragments were isolated from agarose gels with a GeneClean III kit (Bio 101, Vista, Calif.). *E. coli* strains were electroporated with a GenePulser/Pulse Controller (Bio-Rad, Hercules, Calif.) at 15 kV/cm, 25 μF, and 200 Ω.

Saturation mutagenesis. Saturation mutagenesis was performed by using the procedure of Sakamoto et al. (34) with random DNA mutations introduced at the desired positions during PCR. Each 100-μl PCR mixture contained 30 ng of

template DNA, 30 pmol of each primer, 20 nmol of each deoxyribonucleoside triphosphate, and 5 U of *Pfu* DNA polymerase. The PCR program consisted of 30 cycles of 1 min at 94°C, 1 min at 55°C, and 2.5 min at 72°C (with a final extension for 7 min at 72°C). Two primers, T4MOG103A107Front (5′-ATTACGGCGCCATCGCAGTTNNNGAATATGCANNNGTAACCG-3′) and T4MOG103A107Rear (5′-ATACGACCTTCACCGGTTACNNNTGCATATTCNNNAACTGCG-3′) were designed to randomize simultaneously both positions 103 and 107 of TmoA, the alpha subunit of T4MO hydroxylase. Two additional primers used for cloning were T4MOEcoRIFront (5′-TACGGAATTCAAGCTTTTAAACCCCACAGG-3′) and T4MOBglIIRear (5′-TCCAAGCCCAGATCTATCAACGAGCGTTCG-3′) (the EcoRI and BglII restriction enzyme sites are underlined; the BglII site occurs naturally downstream of TmoA positions 103 and 107, and the EcoRI site is upstream of *tmoA* in the multiple cloning site). Two-step saturation mutagenesis was performed to generate the mutations at the desired positions, and pBS(Kan)T4MO was used as the template for the initial PCR. A 386-nucleotide degenerate product was amplified by PCR using primers T4MOEcoRIFront and T4MOG103A107Rear, and a 648-nucleotide degenerate product of *tmoA* was amplified by PCR using primers T4MOG103A107Front and T4MO BglIIRear. After purification with a Wizard PCR purification kit (Promega, Madison, Wis.), the two initial PCR products (50 ng each) were combined and used as the template in the second PCR performed with T4MOEcoRIFront and T4MOBglIIRear to obtain the full-length, degenerate, 981-nucleotide fragment. This product, containing randomized nucleotides at TmoA codons 103 and 107, was cloned into pBS(Kan)T4MO after double digestion with EcoRI and BglII.

Similarly, to generate mutations at the TmoA I100 position, a 366-nucleotide degenerate product was amplified by PCR using primers T4MOEcoRIFront and T4MO100Rear (5′-GCTGCATATTCACCAACTGCNNNGGCGCCGTAATGG-3′), and a 663-nucleotide degenerate product of *tmoA* was amplified by PCR using primers T4MO100Front (5′-CACTTTGAAATCCCATTACGGCGCCNNNGCAGTTGG-3′) and T4MOBglIIRear. As described above, the two initial PCR products were combined to obtain the full-length, degenerate, 981-nucleotide fragment which was cloned into pBS(Kan)T4MO.

Colony screening with nylon membranes. Saturation mutagenesis mutant libraries of *E. coli* TG1/pBS(Kan)T4MO were screened on agar plates containing *o*-methoxyphenol or *o*-cresol by using a modification of a procedure (3, 23) which was based on the enzymatic production of catechols that, upon secretion, autooxidize to red-brown metabolites. Along with the negative control *E. coli* TG1/pBS(Kan) and TG1/pBS(Kan)T4MO, around 50 T4MO transformants were transferred with sterile toothpicks to a single LB medium plate containing 100 μg of kanamycin per ml and 1% glucose for overnight incubation [the glucose served to prevent enzyme production from pBS(Kan)T4MO and to reduce plasmid segregational instability during growth]. The colonies were transferred with a nylon membrane (Osmonics Inc., Minnetonka, Minn.) to an LB medium plate containing 100 μg of kanamycin per ml and 1 mM *o*-methoxyphenol or *o*-cresol. The plates were periodically inspected during a 12- to 24-h incubation period at room temperature. The colonies that had a different color around the cell mass or a more intense color than the wild-type T4MO color were chosen for another round of screening. If positive mutants were detected, the plasmids were isolated and sequenced.

Enzymatic activity. Oxidations of *o*-methoxyphenol, *o*-cresol, *m*-cresol, and *p*-cresol by the wild-type T4MO and the mutants identified from saturation mutagenesis were examined for regiospecificity and product formation rates. One milliliter of a concentrated exponential-phase cell suspension (OD_{600}, 10) in Tris-HCl buffer was mixed with 1 mM substrate (dissolved in 99.5% ethanol) in a 15-ml serum vial sealed with a Teflon-coated septum and an aluminum crimp seal; the large headspace volume (14 ml) ensured that there was ample oxygen for the 1-ml resting cell reaction. The negative controls used in these experiments contained the same monooxygenase without substrate (but with solvent), as well as TG1/pBS(Kan) with substrates (no-monooxygenase control). The inverted vials were shaken at 37°C at 300 rpm on a KS260 shaker (IKA Works, Inc., Wilmington, N.C.), and five to eight samples were taken during 240-min incubations. Each cell suspension was removed and centrifuged in a 16 M Spectrafuge (Labnet, Edison, N.J.) for 2 min. The supernatant was analyzed by high-performance liquid chromatography (HPLC) for product identification and quantification for all the substrates tested. At least three time points from the linear parts of the product formation rate curves or substrate consumption rate curves were used for calculation of specific initial rates. All rates were determined with a protein concentration of 0.24 mg of protein/ml/OD_{600} unit and were expressed as the mean ± standard deviation (based on at least two independent results).

For 3-methoxycatechol determination from *o*-methoxyphenol, the supernatant was also analyzed by using the catechol spectrophotometric method developed previously (42), which is based on the color reaction of catechol, iron(III), and phenylfluorone. The catechol concentration was measured by adding 300 μl of 0.1 M sodium carbonate–0.1 M sodium hydrogen carbonate buffer, 100 μl of 5% polyoxyethelene monolauryl ether (Acros Organics), 60 μl of 1 mM iron(III) ammonium sulfate, 60 μl of 1 mM phenylfluorone (Acros Organics) in methanol, and 380 μl of sterile water to 100 μl of supernatant to obtain a final volume of 1.0 ml in a 1.5-ml microcentrifuge tube. After 1 min, the absorbance of the color complex (catechol-Fe^{III}-phenylfluorone) was measured at 630 nm by using a UVmini-1240 spectrophotometer (Shimadzu, Kyoto, Japan).

To determine the apparent V_{max} and K_m for *o*-, *m*-, and *p*-cresol oxidation by the wild-type T4MO, 1 ml of exponentially grown cells (OD_{600}, 6) was sealed with 25, 50, 75, 150, 250, 500, or 1,000 μM substrate. Samples were analyzed by HPLC after 0 to 30 min of shaking at 300 rpm, and the initial product formation rates for *o*-, *m*-, and *p*-cresol oxidation at the seven different concentrations were calculated. The steady-state kinetic parameters (V_{max} and K_m) were determined from a Lineweaver-Burk double-reciprocal plot.

For toluene oxidation, 2 ml of a concentrated cell suspension (OD_{600}, 5) in Tris-HNO_3 buffer was sealed in a 15-ml serum vial, and 300 μM toluene was added to the vial with a syringe, calculated as if all the substrate was in the liquid phase (the actual initial liquid concentration was 109 μM based on a Henry's Law constant of 0.27 [9]). The inverted vial was shaken at room temperature at 300 rpm. The reaction was stopped by adding 2 ml of 500 μM hexadecane (the internal standard) in ethyl acetate to the vial with a syringe, and the vial was vortexed thoroughly to ensure complete extraction of the toluene. The organic phase was separated from the aqueous phase by centrifugation, and 2 to 3 μl was injected to a gas chromatograph (GC) column.

Analytical methods. Reverse-phase HPLC was conducted to determine the product formation rates and the regiospecificity from *o*-methoxyphenol, *o*-cresol, *m*-cresol, and *p*-cresol oxidation. Supernatants (20 μl) were injected with an autosampler (Waters 717 plus) and were analyzed using a Zorbax SB-C_8 column (5 μm; 4.6 by 250 mm; Agilent Technologies) with a Waters Corporation (Milford, Mass.) 515 solvent delivery system coupled to a photodiode array detector (Waters 996).

When *o*-methoxyphenol was the substrate, isocratic elution was performed with H_2O (0.1% formic acid)-acetonitrile (70:30) as the mobile phase at a flow rate of 1 ml/min in most cases; the exception was G103S, for which gradient elution (85:15 for 0 to 8 min, gradient to 65:35 at 13 min, and gradient to 85:15 at 18 min) was used to obtain better separation of the methoxyhydroquinone and 4-methoxyresorcinol products. For the three cresol substrates, gradient elution was performed with H_2O (0.1% formic acid)-acetonitrile (70:30 for 0 to 8 min, gradient to 40:60 at 15 min, and gradient to 70:30 at 20 min) as the mobile phase. The identities of all products produced by the enzymes were determined by comparing both the retention times and the UV-visible spectra to those of authentic standards and were corroborated by coelution with the standards.

Toluene concentrations were measured by GC by using a Hewlett-Packard 6890N GC equipped with an EC-WAX column (30 m by 0.25 mm; thickness, 0.25 μm; Alltech Associates, Inc., Deerfield, Ill.) and a flame ionization detector. The injector and detector were maintained at 250 and 275°C, respectively, and a split ratio of 3:1 was used. The He carrier gas flow rate was maintained at 0.8 ml/min. The temperature program was 80°C for 5 min, followed by an increase from 80 to 205°C at a rate of 5°C/min, an increase from 205 to 280°C at a rate of 15°C/min, and 280°C for 5 min. Under these conditions, toluene, *o*-cresol, *p*-cresol, and *m*-cresol eluted at 4.2, 27.4, 29.1, and 29.3 min, respectively, while the internal standard hexadecane eluted at 17.8 min. Retention times were determined by comparisons to authentic standards.

DNA sequencing. A dideoxy chain termination technique (36) performed with an ABI Prism BigDye Terminator Cycle Sequencing Ready Reaction kit (Perkin-Elmer, Wellesley, Mass.) and a PE Biosystems ABI 373 DNA sequencer (Perkin-Elmer) was used to determine the nucleotide sequence in the subcloned region for the T4MO enzyme variants by using T4MOEcoRIFront as the sequencing primer. The sequence data generated were analyzed with the Vector NTI software (InfoxMax, Inc., Bethesda, Md.).

TmoA modeling. Amino acids 44 to 243 of the T4MO alpha-subunit TmoA (500 amino acids) were modeled into the known three-dimensional structure of the *Methylococcus capsulatus* (Bath) soluble methane monooxygenase (sMMO) hydroxylase α-subunit MmoX (PDB accession code 1MTY) by using the SWISS-MODEL Server (13, 27, 38). The molecular visualization program Swiss-PdbViewer was utilized to visualize the molecular model and to perform amino acid substitutions isosterically at TmoA I100, G103, and A107 based on residue interactions, steric hindrance, and energy minimization.

TABLE 1. Toluene oxidation rates and regiospecificity for TG1 expressing wild-type T4MO and saturation mutagenesis TmoA variants[a]

Enzyme	Toluene oxidation rate (nmol/min/mg of protein)	Regiospecificity (%)		
		p-Cresol	*m*-Cresol	*o*-Cresol
Wild-type T4MO	12.1 ± 0.8	96	3	<1
I100L	17.7 ± 0.2	90	3	7
G103A	20.1 ± 0.4	75	13	12
G103A/A107S	18.2 ± 1.6	71	17	12
G103L[b]		25	20	55
G103S	18.1 ± 1.7	76	15	9
G103S/A107G	1.5 ± 0.3	11	7	82
G103S/A107T	2.5 ± 0.4	100	0	0

[a] The initial toluene concentration in the liquid phase was 109 μM based on a Henry's Law constant of 0.27 (9) (300 μM if all the toluene was contained in the liquid phase). The rate data are means ± standard deviations based on at least two independent experiments.

[b] Purified enzyme from a previous study (25). The mutant was created by site-directed mutagenesis and had 64% of the toluene oxidation activity of wild-type T4MO.

RESULTS

Oxidation of toluene, *o*-cresol, *m*-cresol, and *p*-cresol by wild-type T4MO. A whole-cell system was used to oxidize substrates due to the multiple components of T4MO (hydroxylase, reductase, mediating protein, and ferredoxin) and its dependence on the cofactor NADH. Recombinant TG1/pBS(Kan)T4MO cells oxidized toluene to 96% *p*-cresol, 3% *m*-cresol, and less than 1% *o*-cresol (Table 1), giving a product distribution nearly identical to that of the purified T4MO (96.0% *p*-cresol, 0.4% *o*-cresol, 2.8% *m*-cresol, and 0.8% benzyl alcohol) (29). The negative control *E. coli* TG1/pBS(Kan) did not produce any product from the substrates tested (*o*-methoxyphenol and cresols) and did not degrade any dihydroxylated compounds in the time scale of these experiments; hence, the products were formed due to hydroxylation by the cloned T4MO.

Based on the recent discovery that T4MO successively hydroxylates benzene to phenol, catechol, and 1,2,3-trihydroxybenzene (42), wild-type T4MO was investigated here for its activity with cresols and was found to hydroxylate them to methylcatechols, further indicating that T4MO can hydroxylate phenols. All three cresol isomers were utilized and transformed by wild-type T4MO to corresponding catechols at significant concentrations. Kinetic analysis of *o*-, *m*-, and *p*-cresol oxidation by wild-type T4MO showed that this enzyme follows typical saturation kinetics with these three cresol substrates; the apparent V_{max} and K_m values were 7.6 ± 2.2 nmol/min/mg of protein and 0.13 ± 0.05 mM, respectively, for 3-methylcatechol formation from *o*-cresol, 10.7 ± 0.1 nmol/min/mg of protein and 0.18 ± 0.01 mM, respectively, for 4-methylcatechol formation from *m*-cresol, and 6.6 ± 0.9 nmol/min/mg of protein and 0.18 ± 0.02 mM, respectively, for 4-methylcatechol formation from *p*-cresol. The rates of methylcatechol formation were similar to the oxidation rate of the physiological substrate, toluene (the apparent V_{max} of toluene oxidation for wild-type T4MO was 15.1 ± 0.8 nmol/min/mg of protein [10]); hence, the rates of methylcatechol formation are significant.

The substrate (cresol) oxidation rates and dihydroxylated product formation rates compared well and are shown in Table 2. HPLC analysis showed that TG1 expressing wild-type T4MO oxidized *o*-methoxyphenol to 4-methoxyresorcinol (87%), 3-methoxycatechol (11%), and methoxyhydroquinone (2%); oxidized *o*-cresol to 3-methylcatechol (91%) and methylhydroquinone (9%); and oxidized *m*-cresol and *p*-cresol to 4-methylcatechol (100%) (Tables 2 and 3 and Fig. 1).

Saturation mutagenesis of T4MO. Codon I100 of TmoA was mutated independently, and codons G103 and A107 were mutated together by using saturation mutagenesis. Libraries of 1,000 clones for I100 and 600 clones for G103/A107 were obtained after saturation mutagenesis. A total of 300 clones from the I100 library and 350 clones from the G103/A107 library were screened to ensure that the probability that all 64 possible codons from the single and double sites were checked was 99% (32).

A rapid nylon membrane plate assay was used to screen for the production of catechol derivatives from the TG1/pBS(Kan)T4MO mutants. Pure substituted catechols synthesized in this study were also tested on the nylon membranes; 3-methoxycatechol and methoxyhydroquinone rapidly produced red spots on the nylon membrane (within 2 h), but 4-methoxyresorcinol did not produce color on the nylon membrane even after a longer incubation time (24 h). The mutants identified that produced the various methoxy-substituted catechols from *o*-methoxyphenol reflect the validity and limitations of this nylon membrane screening approach in that 3-methoxycatechol syn-

TABLE 2. Cresol hydroxylation and synthesis of dihydroxylated products (3-methylcatechol, 4-methylcatechol, and methylhydroquinone) by *E. coli* TG1 expressing wild-type T4MO and saturation mutagenesis TmoA variants[a]

Enzyme	Substrate	Regiospecificity (%)			Formation rate (nmol/min/mg of protein)			Cresol oxidation rate (nmol/min/mg of protein)
		3-Methylcatechol	Methylhydroquinone	4-Methylcatechol	3-Methylcatechol	Methylhydroquinone	4-Methylcatechol	
Wild type	*m*-Cresol	0	0	100	0	0	9.5 ± 1.3	10.4 ± 0.1
Wild type	*p*-Cresol	0	0	100	0	0	6.0 ± 1.1	7.9 ± 1.6
Wild type	*o*-Cresol	91	9	0	6.7 ± 2.2	0.5 ± 0.2	0	8.9 ± 2.8
G103A	*o*-Cresol	96	4	0	6.2 ± 3.1	0.11	0	6.3 ± 3.1
G103A/A107S	*o*-Cresol	98	2	0	13.4 ± 0.1	0	0	14.5 ± 2.1
G103S	*o*-Cresol	20	80	0	0.30 ± 0.02	2.1 ± 0.1	0	4.1 ± 0.3
G103S/A107G	*o*-Cresol	30	70	0	0.08 ± 0.03	0.34 ± 0.02	0	0.4 ± 0.1
G103S/A107T	*o*-Cresol	8	92	0	0.16 ± 0.02	2.1 ± 0.7	0	2.3 ± 0.4

[a] Based on HPLC analysis. The rate data are means ± standard deviations based on at least two independent experiments. Activity was determined at a saturation substrate concentration of 1 mM.

TABLE 3. 3-Methoxycatechol, methoxyhydroquinone, and 4-methoxyresorcinol synthesis from *o*-methoxyphenol by *E. coli* TG1 expressing wild-type T4MO and saturation mutagenesis TmoA variants[a]

Enzyme	Regiospecificity of *o*-methoxyphenol oxidation (%)			3-Methoxycatechol formation rate (nmol/min/mg of protein)			Methoxyhydroquinone formation rate (nmol/min/mg of protein)[c]	*o*-Methoxyphenol oxidation (nmol/min/mg of protein)
	4-Methoxyresorcinol	3-Methoxycatechol	Methoxyhydroquinone	Via HPLC	Relative activity[b]	Via colorimetric assay		
Wild type	87	11	2	0.21 ± 0.01	1	0.2	0.07 ± 0.03	4.1 ± 1.1
I100L	73	20	7	0.8 ± 0.2	4	0.9–1.3	~0	2.4 ± 0.8
G103A	41	52	7	1.2 ± 0.2	6	0.7–2.7	~0	2.1 ± 0.5
G103A/A107S	13	82	5	1.5 ± 0.2	7	1.9	~0	1.9
G103S	19	<1	80	~0	0	0	0.36 ± 0.01	0.4
G103S/A107T	35	30	35	ND[d]	0	0	0.08	ND

[a] Activity was determined at a saturation substrate concentration of 1 mM.
[b] Relative values based on HPLC analysis. The colorimetric assay corroborated the data.
[c] The *o*-methoxyphenol substrate was oxidized to as many as three different products, but only the methoxyhydroquinone formation rate is shown.
[d] ND, not determined.

thesis and methoxyhydroquinone synthesis were favored over 4-methoxyresorcinol synthesis. Using pure 4-methoxyresorcinol, we found that the quinone from the oxidized 4-methoxyresorcinol product (the source of the red color) was difficult to see on the nylon membrane.

Three clones identified from the nylon screen assay on *o*-methoxyphenol LB medium plates containing kanamycin from the TmoA I100 mutant library were sequenced and contained the same amino acid substitution, I100L. Seven clones from the TmoA G103/A107 mutant library were selected after two rounds of nylon screening with LB medium plates containing *o*-methoxyphenol and kanamycin, and sequencing revealed that four different enzymes were created: TmoA G103A, G103S, G103S/A107T, and G103A/A107S. TmoA G103S was identified four times by this screening procedure. For *o*-cresol, three clones from the TmoA G103/A107 mutant library of 100 mutants were selected based on the different colors that developed on the nylon membrane and were sequenced. Wild-type T4MO produced a yellow halo on the nylon membranes, while the mutant enzymes produced a red halo. Two types of enzymes were found; one mutant was found to have G103S/A107G substitutions, and two mutants were found to have the same substitution as G103S.

3-Methoxycatechol-producing mutants were further identified by a catechol colorimetric assay following the nylon membrane *o*-methoxyphenol plate assay since both the methoxyhydroquinone- and 3-methoxycatechol-synthesizing mutants produced a red color on the nylon membrane plate containing *o*-methoxyphenol. This catechol colorimetric assay has been used previously for catechol detection from benzene (42); however, it should be noted that the colorimetric assay for 3-methoxycatechol is not as sensitive as the assay for catechol and cannot detect methoxyhydroquinone, but it corroborated the HPLC rates well (see below). Mutants I100L, G103A, and G103A/A107S had enhanced 3-methoxycatechol synthesis from *o*-methoxyphenol, and the specific activities determined by the colorimetric assay are shown in Table 3. There was a 3- to 14-fold increase in the activity of 3-methoxycatechol formation compared to the wild-type T4MO activity. Mutants G103S and G103S/A107T had a dark brown color on the nylon membrane but did not show 3-methoxycatechol synthesis activity when the colorimetric assay was used. Thus, these two mutants were initially identified as methoxyhydroquinone-producing mutants.

Oxidation of toluene by the saturation mutagenesis variants. Six saturation mutagenesis TmoA mutants (I100L, G103A, G103S, G103A/A107S, G103S/A107G, and G103S/A107T) were characterized both for their initial specific activities and for their monohydroxylation regiospecificities on the natural substrate toluene (Table 1). These mutants had initial specific activities for toluene oxidation comparable to that of wild-type T4MO (21 to 166% of wild-type T4MO activity), demonstrating that most of the mutants were effective aromatic catalysts; the only exception was G103S/A107G, for which the oxidation activity with toluene was 12% of the wild-type activity. However, taking into account the lower expression level of the G103S/A107G variant enzyme (see below), this mutant showed significant activity with toluene and the other substrates. These results also indicate that it is possible to increase the rate of toluene oxidation beyond that of the wild-type enzyme but that this occurs at the expense of reduced regiospecificity.

T4MO site-directed mutant TmoA G103L was reported previously to produce 55% *o*-cresol from toluene oxidation (25). Here, regiospecific oxidation of toluene was observed with the TmoA saturation mutagenesis mutants that were identified by the nylon membrane assay. In particular, G103S/A107G and G103S/A107T produced 82% *o*-cresol and 100% *p*-cresol, respectively; therefore, the mutations completely changed the nature of toluene oxidation by T4MO, converting the enzyme to T2MO and an even better T4MO. Moreover, toluene oxidation by the other saturation mutagenesis mutants (I100L, G103A, G103S, and G103A/A107S) resulted in elevated yields of *ortho*- and *meta*-monohydroxylation products relative to the yields obtained with wild-type T4MO.

Oxidation of *o*-cresol, *m*-cresol, and *p*-cresol by the saturation mutagenesis variants. TmoA variants G103S/A107G, G103S, G103A, G103A/A107S, and G103S/A107T were characterized by HPLC to determined the product formation rates and the regiospecificities at a cresol concentration of 1 mM since this concentration was found to be in the saturated range for *o*-cresol, *m*-cresol, *p*-cresol, and *o*-methoxyphenol oxidation by wild-type T4MO and no substrate inhibition was seen; also, 1 mM is at least five times greater than the apparent K_m values for these substrates.

These variants exhibited *o*-cresol oxidation rates comparable to the wild-type T4MO rate, while the product distributions were

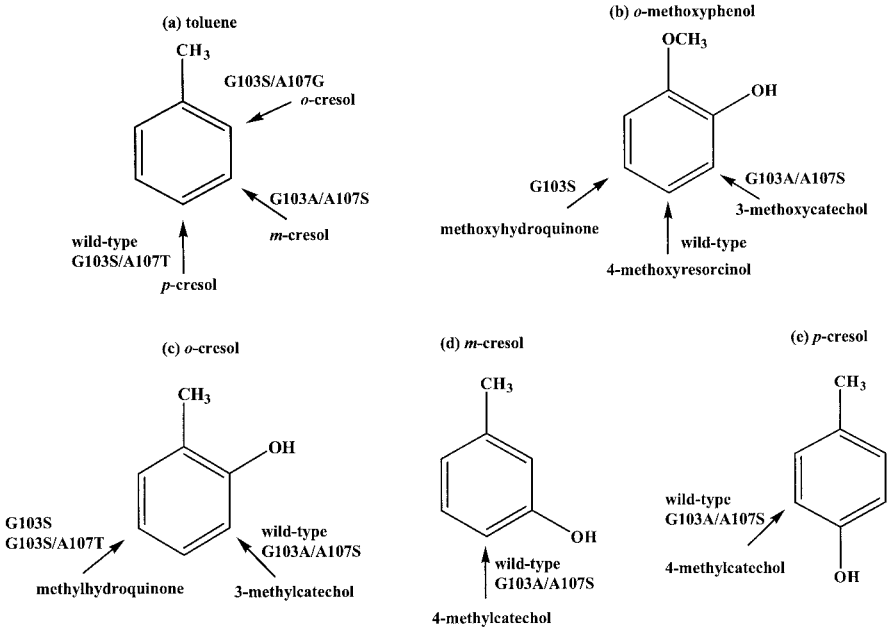

FIG. 1. Positions of hydroxylation of toluene, *o*-methoxyphenol, and cresols by wild-type T4MO and the TmoA variants. The arrows indicate the sites of hydroxylation. The resulting products and the responsible enzymes are also indicated.

changed substantially (Table 2 and Fig. 1). Mutants G103S, G103S/A107G, and G103S/A107T oxidized *o*-cresol to 70 to 92% methylhydroquinone, values which are 8 to 10 times higher than the methylhydroquinone percentage obtained with wild-type T4MO (Table 2). In addition, the rates of methylhydroquinone formation by mutants G103S and G103S/A107T were more than four times higher than the wild-type T4MO rate. On the other hand, G103A and G103A/A107S produced 96 and 98% 3-methylcatechol from *o*-cresol, respectively, while 91% 3-methylcatechol was observed with the wild-type T4MO. The specific rates of formation of 3-methylcatechol by G103A and G103A/A107S were 92 and 216% of the specific rate of formation of 3-methylcatechol by wild-type T4MO, respectively (Table 2). As observed with wild-type T4MO, the substrate (*o*-cresol) depletion rates agreed well with the measured product formation rates.

With the substrates *m*-cresol and *p*-cresol, T4MO variants G103S, G103A/A107S, and G103S/A107T produced 4-methylcatechol, the same product that wild-type T4MO produced (Table 2 and Fig. 1). The 4-methylcatechol formation rates for G103S and G103A/A107S were comparable to the 4-methylcatechol formation rates for wild-type T4MO for both substrates (59 and 88% of the wild-type activity with 1 mM *m*-cresol, respectively, and 94 and 148% of the wild-type activity with 1 mM *p*-cresol, respectively), while G103S/A107T showed reduced *m*-cresol and *p*-cresol oxidation activities (15 and 4% of the wild-type activities, respectively).

Oxidation of *o*-methoxyphenol by the saturation mutagenesis variants. The best mutants identified from *o*-methoxyphenol oxidation by the nylon membrane assay and colorimetric assay, T4MO TmoA I100L, G103A, G103A/A107S, and G103S, were further examined by HPLC and were found to make different regiospecific products from *o*-methoxyphenol (Table 3 and Fig. 1); HPLC also was used to corroborate the initial 3-methoxycatechol formation rates determined by the colorimetric assay and to confirm the possible product identities based on the nylon membrane assay and catechol colorimetric assay. G103A synthesized 3-methoxycatechol six times faster than wild-type T4MO (Table 3) and had an increased regiospecificity for 3-methoxycatechol formation (52%). Notably, G103A/A107S produced primarily 3-methoxycatechol (82%), and the rate of synthesis was more than seven times higher than the rate of synthesis by the wild-type enzyme (Table 3) because of the additional mutation A107S.

I100L was found to have nearly unchanged regiospecificity for *o*-methoxyphenol oxidation and produced predominantly 4-methoxyresorcinol (73%). The second major product, 3-methoxycatechol, was made at a rate that was nearly four times higher than the rate of production by wild-type T4MO. The specific activities for 3-methoxycatechol formation determined by HPLC analysis corroborated the results of the colorimetric assay (Table 3). It appears that the I100 position does not affect regiospecificity very much (Table 1 and Table 3).

In contrast, two mutants, G103S and G103S/A107T, produced methoxyhydroquinone as a major product (80 and 35%, respectively) from *o*-methoxyphenol, whereas wild-type T4MO produced only trace amounts of methoxyhydroquinone (Table 3). G103S synthesized methoxyhydroquinone at a rate that was fivefold greater than the wild-type T4MO rate, and there was a 40-fold increase in the percentage of methoxyhydroquinone formed compared to the wild-type T4MO value (Table 3). G103S/A107T produced the new product methoxyhydroquinone at the same rate as the wild-type enzyme, while the regiospecificity was changed.

Protein expression level and specific growth rate. By using sodium dodecyl sulfate-polyacrylamide gel electrophoresis, the T4MO α-subunit TmoA (55 kDa) and the β-subunit TmoE (36 kDa) were visualized on gels for both the mutant and wild-type enzymes. The expression levels of the proteins were found to

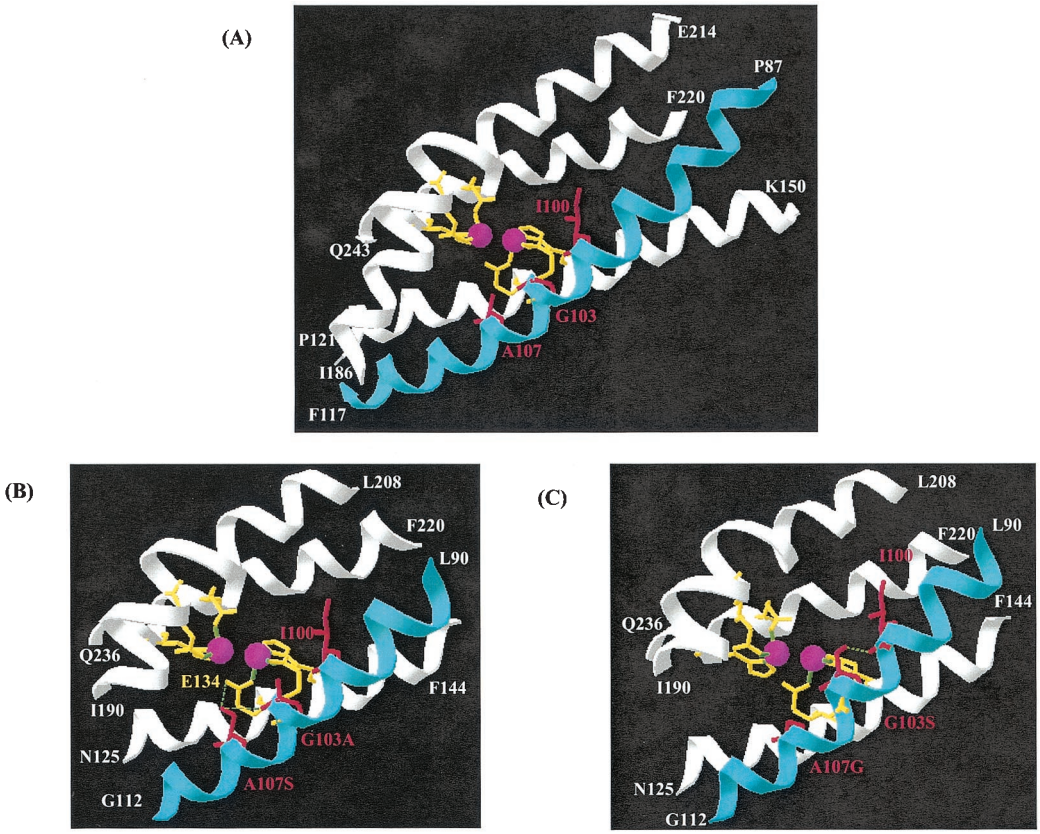

FIG. 2. Active sites of the T4MO α-subunit TmoA, showing mutations (red) at positions G103 and A107. (A) Wild-type I100, G103, and A107; (B) G103A/A107S with putative hydrogen bonds to the carbonyl of A103 or E134 (dashed green lines); (C) G103S/A107G with a putative hydrogen bond to the carbonyl of I100 (dashed green line). Yellow residues (E104, E134, H137, E197, E231, and H234) are coordinate residues anchoring the diiron-binding sites (pink spheres). The four-helix bundle of TmoA (helix B, P87-F117; helix C, P121-K150; helix E, I186-E214; and helix F, F220-Q243) anchoring the diiron active site is shown in white in panel A, and portions of the four-helix bundle are shown in white terminating at L90-G112 (helix B), N125-F144 (helix C), I190-L208 (helix E), and F220-Q236 (helix F) in panels B and C.

remain approximately constant for mutants I100L, G103A, G103A/A107S, G103S, and G103S/A107T, while the expression levels for G103S/A107G were only one-third the expression levels for wild-type T4MO proteins. However, all variants showed significant expression of TmoA and TmoE and significant oxidation activity on substituted benzene substrates (see above). Variant I100L grew at nearly the same rate as the wild type (1.34 ± 0.01 and 1.14 ± 0.03 h^{-1}, respectively, in LB medium containing kanamycin). As the cell growth and biotransformation conditions were identical for the wild type and mutants, the changes in catalytic properties (rates and regiospecificities) arose from the mutations in TmoA at positions I100, G103, and A107 and not from different expression levels.

TmoA structure homology modeling. To assess the effects of the amino acid substitutions at positions I100, G103, and A107 on the T4MO catalytic properties, an approximate three-dimensional model was constructed based on the known crystal structure of MmoX hydroxylase of sMMO (30) (Fig. 2). sMMO consists of an $(\alpha\beta\gamma)_2$ hydroxylase, a reductase, a coupling protein, and an open reading frame (OrfY), and each α subunit of hydroxylase contains one diiron center (8). At the diiron center, oxygen is activated, and substrate hydroxylation coupled to NADH oxidation occurs (17). Although TmoA and MmoX (the large subunits of T4MO and sMMO, respectively) exhibit only 27% amino acid identity and there are limitations to homology modeling with low levels of identity (12), the correct fold was generated, as judged by the positions of the diiron coordinating residues in T4MO (E104, E134, H137, E197, E231, and H234) compared to those in sMMO (30, 31); the root mean square deviation between the corresponding C_α of the six coordinates of the TmoA model and template sMMO model was 0.07 Å. The structural alignment of the template and model also showed conserved spatial configurations.

The model helped us to visualize the locations of the mutations and the side chains of G103S, A107S, A107G, and A107T (Fig. 2). The TmoA model showed that mutated residues I100, G103, and A107 lie in a very closed region of the same α-helix (helix B) of the four-helix bundle of TmoA (since all three residues are separated by 4 amino acids, they appear to be on roughly the same side of the helix) and are near the diiron center (Fig. 2A). I100 and A107 are constituents of this hydrophobic pocket (residues F205, I227, I224, I100, F176, A107, I180, L192, F196, and T201) (30, 31), and the alanine residue at TmoA position 107 is conserved in all monooxygenases, including sMMO, TOM, toluene/*o*-xylene monooxygenase, and toluene *para*-monooxygenase of *R. pickettii* (18). G103 is adjacent to the Fe-coordinating residue E104.

DISCUSSION

It was reported previously that no catechol derivatives were detected by using T4MO with toluene and benzene as substrates (29), and recently Mitchell et al. (25) also reported that there was no further hydroxylation of *p*-cresol by the T4MO G103L mutant created by site-directed mutagenesis. All previous publications indicated that T4MO hydroxylates only unactivated benzene nuclei and not phenolic compounds (18, 25, 29). However, it was discovered recently in our laboratory that T4MO produces catechol at physiological rates by using both benzene and phenol as substrates (42). Not surprisingly, 3-methylcatechol, 4-methylcatechol, and methylhydroquinone were found here to form from the oxidation of *o*-, *m*-, and *p*-cresol. Thus, these findings not only correct the misunderstanding that wild-type T4MO can hydroxylate only benzenes to monohydroxylated products and cannot subsequently hydroxylate phenols (18) but also show that wild-type T4MO is a good biocatalyst for making some industrially significant, substituted, catecholic compounds.

TmoA I100, G103, and A107 were chosen as possible hot spots for active-site engineering based on studies with T4MO and a related toluene monooxygenase (6, 25, 32a; Fox, 102nd Gen. Meet. Am. Soc. Microbiol.), in which regiospecific changes or enhanced activities were discovered at analogous sites by using toluene, indole, or naphthalene substrates. None of these studies considered more than single hydroxylations; however, regiospecific synthesis of dihydroxylated compounds is a rather important application of these monooxygenases in addition to their use in environmental remediation (7, 11, 21, 33, 39, 41). Saturation mutagenesis is useful and efficient for fine-tuning a protein by accumulation of beneficial mutations if active sites have been identified, and here we used this approach on T4MO TmoA at positions I100, G103, and A107.

Some of the TmoA variants obtained exhibited altered regiospecificity for toluene, *o*-cresol, and *o*-methoxyphenol. Variants with the G103S substitution (with an A, T, or G residue at position 107) all favored methylhydroquinone synthesis from *o*-cresol rather than the synthesis of 91 to 98% 3-methylcatechol observed with wild-type T4MO, G103A, and G103A/A107S (Table 2). In addition, the G103S and G103S/A107T variants both formed methoxyhydroquinone from *o*-methoxyphenol (Table 3). It appears that mutation G103S in TmoA is responsible for the methylhydroquinone and methoxyhydroquinone formation. Furthermore, the nearly perfect 3-methylcatechol-synthesizing enzyme G103A/A107S (Table 2) exhibited an ability to form high percentages of 3-methoxycatechol from *o*-methoxyphenol as well (Table 3). Thus, for *o*-cresol and *o*-methoxyphenol, these mutants demonstrated the same regiospecific second hydroxylation (unlike wild-type T4MO).

In contrast, the G103S substitution did not affect significantly the regiospecificity of toluene monohydroxylation. T4MO is a highly specific enzyme for *para* hydroxylation of toluene, nitrobenzene, and methoxybenzene. It was not surprising to observe relaxed toluene oxidation with the TmoA I100 and G103 variants here since nature has tuned T4MO for highly regiospecific synthesis of *p*-cresol, which is converted to the intermediates *p*-hydroxybenzaldehyde and *p*-hydroxybenzoate, which are transformed to protocatechuate (43). In contrast to G103S, the *ortho*-hydroxylating enzyme (G103S/A107G) and perfect *para*-hydroxylating enzymes (G103S/A107T) suggest that TmoA A107 controls the regiospecific oxidation of toluene at the level of monohydroxylation. This corroborates the finding that TOM TomA3 A113 (analogous to TmoA A107) is responsible for regiospecific oxidation of indole (32a).

The effects of the G103S and A107S mutations on *o*-cresol and *o*-methoxyphenol oxidation and the effects of the A107G and A107T substitutions on toluene monohydroxylation are not apparent considering the discrepancy between toluene and *o*-cresol oxidation regiospecificities; however, the structural model of T4MO TmoA indicates that the hydroxyl residue of Ser in variant G103S may form an additional hydrogen bond with the carbonyl of I100 (Fig. 2C) and the hydroxyl residue of Ser107 in the double-mutation variant G103A/A107S may form an additional hydrogen bond with the carbonyl of A103 and with the carbonyl of the Fe-coordinating residue E134 (Fig. 2B). In addition, the hydroxyl of A107T in variant G103S/A107T may form a hydrogen bond with the carbonyl of S103. Furthermore, the replacement of G103 and A107 by hydroxyl-group-containing residues (Ser or Thr) may lead to the formation of a hydrogen bond with the hydroxyl moiety of the phenolic substrates which may orient the substrate for attack at the *ortho* or *para* positions (e.g., G103A/A107S and G103S with *o*-methoxyphenol and *o*-cresol). The importance of hydrogen bonding for protein function has been shown in many cases. For example, in phenol 2-monooxygenase from *Trichosporon cutaneum*, Y289 was reported to play an important role in leading to *ortho* attack of the substrate by forming a hydrogen bond with phenol substrate (23, 44), and the thermophilic xylose isomerase from *Clostridium thermosulfurogenes* increased the k_{cat} for glucose by 38% with an additional hydrogen bond to the C_6-OH group of the substrate upon the mutation V186T (22). In addition, disruption of hydrogen bonds may cause the important amino acids in the catalytic site to lose their catalytic activity (2, 19). The formation of additional hydrogen bonds with the backbone carbonyl, Fe-coordinating carbonyl, and with the substrates here may cause the substrate to be oriented in a different position, and this may explain the altered regiospecificity of oxidation for *o*-cresol and *o*-methoxyphenol by these mutants. This hypothesis is consistent with the results obtained for variant G103S/A107G, whose toluene oxidation was altered to favor *o*-cresol formation due to the addition of A107G to the G103S mutant, while the addition of A107G did not contribute much to *o*-cresol oxidation regiospecificity for G103S/A107G due to its inability to form additional hydrogen bonds with *o*-cresol. The G103S/A107G model (Fig. 2C) indicates that replacement of alanine by the even smaller residue glycine in A107G enlarges the substrate-binding pocket around the diiron center; hence, perhaps the *ortho* position on the aromatic substrate ring near the methyl group may be closer to the diiron center and then oxidation at the *ortho* position of toluene takes place.

In conclusion, mutants capable of specifically synthesizing 3-methylcatechol, methylhydroquinone, methoxyhydroquinone, and 3-methoxycatechol with high efficiency were discovered. Therefore, six dihydroxylated products (82% 3-methoxycatechol, 87% 4-methoxyresorcinol, 80% methoxyhydroquinone, 98% 3-methylcatechol, 100% 4-methylcatechol, and 92% methylhydroquinone) may be synthesized with high purity by a single T4MO enzyme and its variants via a

one-step reaction. On the basis of the observed catalytic activity and product distribution for toluene, *o*-cresol, and *o*-methoxyphenol, we concluded that G103 and A107 are part of the substrate-binding pocket and that T4MO TmoA positions G103S and A107S have a significant role in orienting the substrate for attack at regioselective positions of these phenol substrates. We are investigating the influence of these beneficial mutations with other related monooxygenases.

ACKNOWLEDGMENTS

This research was supported by the National Science Foundation (grant BES-0124401) and the U.S. Environmental Protection Agency.

REFERENCES

1. **Arnold, F. H.** 2001. Combinatorial and computational challenges for biocatalyst design. Nature **409:**253–257.
2. **Bainbridge, G., P. J. Anralojc, P. J. Madgwick, J. E. Pitts, and M. A. J. Parry.** 1998. Effect of mutation of lysine-128 of the large subunit of ribulose bisphosphate carboxylase/oxygenase from *Anacystis nidulans.* Biochem. J. **336:**387–393.
3. **Barriault, D., M.-M. Plante, and M. Sylvestre.** 2002. Family shuffling of a targeted *bphA* region to engineer biphenyl dioxygenase. J. Bacteriol. **184:** 3794–3800.
4. **Bertoni, G., M. Martino, E. Galli, and P. Barbieri.** 1998. Analysis of the gene cluster encoding toluene/*o*-xylene monooxygenase from *Pseudomonas stutzeri* OX1. Appl. Environ. Microbiol. **64:**3626–3632.
5. **Bui, V. P., T. V. Hansen, Y. Stenstrom, and T. Hudlicky.** 2000. Direct biocatalytic synthesis of functionalized catechols: a green alternative to traditional methods with high effective mass yield. Green Chem. **2:**263–265.
6. **Canada, K. A., S. Iwashita, H. Shim, and T. K. Wood.** 2002. Directed evolution of toluene *ortho*-monooxygenase for enhanced 1-naphthol synthesis and chlorinated ethene degradation. J. Bacteriol. **184:**344–349.
7. **Chauhan, S., P. Barbieri, and T. K. Wood.** 1998. Oxidation of trichloroethylene, 1,1,-dichloroethylene, and chloroform by toluene/*o*-xylene monooxygenase from *Pseudomonas stutzeri* OX1. Appl. Environ. Microbiol. **64:**3023–3024.
8. **Coufal, D. E., J. L. Blazyk, D. A. Whittington, W. W. Wu, A. C. Rosenzweig, and S. J. Lippard.** 2000. Sequencing and analysis of the *Methylococcus capsulatus* (Bath) soluble methane monooxygenase genes. Eur. J. Biochem. **267:**2174–2185.
9. **Dolfing, J., A. J. van den Wijngaard, and D. B. Janssen.** 1993. Microbiological aspects of the removal of chlorinated hydrocarbons from air. Biodegradation **4:**261–282.
10. **Fishman, A., Y. Tao, and T. K. Wood.** 2004. Toluene 3-monooxygenase of *Ralstonia pickettii* PKO1 is a *para*-hydroxylating enzyme. J. Bacteriol. **186:** 3117–3123.
11. **Folsom, B. R., and P. J. Chapman.** 1991. Performance characterization of a model bioreactor for the biodegradation of trichloroethylene by *Pseudomonas cepacia* G4. Appl. Environ. Microbiol. **57:**1602–1608.
12. **Guex, N., A. Diemand, and M. C. Peitsch.** 1999. Protein modeling for all. Trends Biochem. Sci. **24:**364–367.
13. **Guex, N., and M. C. Peitsch.** 1997. SWISS-MODEL and the Swiss-PdbViewer: an environment for comparative protein modeling. Electrophoresis **18:**2714–2723.
14. **Held, M., W. Suske, A. Schmid, K.-H. Engesser, H.-P. E. Kohler, B. Witholt, and M. G. Wubbolts.** 1998. Preparative scale production of 3-substituted catechols using a novel monooxygenase from *Pseudomonas azelaica* HBP1. J. Mol. Catal. B Enzym. **5:**87–93.
15. **Hisaindee, S., and D. L. J. Clive.** 2001. A synthesis of puraquinonic acid. Tetrahedron Lett. **42:**2253–2255.
16. **Hua, D. H., M. Tamura, X. Huang, H. A. Stephany, B. A. Helfrich, E. M. Perchellet, B. J. Sperfslage, J.-P. Perchellet, S. Jiang, D. E. Kyle, and P. K. Chiang.** 2002. Syntheses and bioactivities of substituted 9,10-dihydro-9,10-[1,2] benzenoanthracene-1,4,5,8-tetrones. Unusual reactivities with amines. J. Org. Chem. **67:**2907–2912.
17. **Kopp, D. A., and S. J. Lippard.** 2002. Soluble methane monooxygenase: activation of dioxygen and methane. Curr. Opin. Chem. Biol. **6:**568–576.
18. **Leahy, J. G., P. J. Batchelor, and S. M. Morcomb.** 2003. Evolution of the soluble diiron monooxygenases. FEMS Microbiol. Rev. **27:**449–479.
19. **Low, D. W., and M. G. Hill.** 2000. Backbone-engineered high-potential iron proteins: effects of active-site hydrogen bonding on reduction potential. J. Am. Chem. Soc. **2000:**11039–11040.
20. **Macias, F. A., D. Marin, D. Chinchilla, and J. M. G. Molinillo.** 2002. First total synthesis of (+/-)-helibisabonol A. Tetrahedron Lett. **43:**6417–6420.
21. **McClay, K., B. G. Fox, and R. J. Steffan.** 1996. Chloroform mineralization by toluene-oxidizing bacteria. Appl. Environ. Microbiol. **62:**2716–2722.
22. **Meng, M., C. Lee, M. Bagdasarian, and J. G. Zeikus.** 1991. Switching substrate preference of the thermophilic xylose isomerase from D-xylose to D-glucose by redesigning the substrate binding pocket. Proc. Natl. Acad. Sci. USA **88:**4015–4019.
23. **Meyer, A., A. Schmid, M. Held, A. H. Westphal, M. Rothlisberger, H.-P. E. Kohler, W. J. H. van Berkel, and B. Witholt.** 2002. Changing the substrate reactivity of 2-hydroxybiphenyl 3-monooxygenase from *Pseudomonas azelaica* HBP1 by directed evolution. J. Biol. Chem. **277:**5575–5582.
24. **Mitchell, K. H., C. E. Rogge, T. Gierahn, and B. G. Fox.** 2003. Insight into the mechanism of aromatic hydroxylation by toluene 4-monooxygenase by use of specifically deuterated toluene and *p*-xylene. Proc. Natl. Acad. Sci. USA **100:**3784–3789.
25. **Mitchell, K. H., J. M. Studts, and B. G. Fox.** 2002. Combined participation of hydroxylase active site residues and effector protein binding in a *para* to *ortho* modulation of toluene 4-monooxygenase regiospecificity. Biochemistry **41:**3176–3188.
26. **Newman, L. M., and L. P. Wackett.** 1995. Purification and characterization of toluene 2-monooxygenase from *Burkholderia cepacia* G4. Biochemistry **34:** 14066–14076.
27. **Peitsch, M. C.** 1995. Protein modeling by e-mail. Bio/Technology **13:**658–660.
28. **Pikus, J. D., K. H. Mitchell, J. M. Studts, K. McClay, R. J. Steffan, and B. G. Fox.** 2000. Threonine 201 in the diiron enzyme toluene 4-monooxygnease is not required for catalysis. Biochemistry **39:**791–799.
29. **Pikus, J. D., J. M. Studts, K. McClay, R. J. Steffan, and B. G. Fox.** 1997. Changes in the regiospecificity of aromatic hydroxylation produced by active site engineering in the diiron enzyme toluene 4-monooxygenase. Biochemistry **36:**9283–9289.
30. **Rosenzweig, A. C., H. Brandstetter, D. A. Whittington, P. Nordlund, S. J. Lippard, and C. A. Frederick.** 1997. Crystal structures of the methane monooxygenase hydroxylase from *Methylococcus capsulatus* (Bath): implications for substrate gating and component interactions. Proteins Struct. Funct. Genet. **29:**141–152.
31. **Rosenzweig, A. C., C. A. Frederick, S. J. Lippard, and P. Nordlund.** 1993. Crystal structure of a bacterial non-haem iron hydroxylase that catalyses the biological oxidation of methane. Nature **366:**537–543.
32. **Rui, L., Y. M. Kwon, A. Fishman, K. F. Reardon, and T. K. Wood.** 2004. Saturation mutagenesis of toluene *ortho*-monooxygenase for enhanced 1-naphthol synthesis and chloroform degradation. Appl. Environ. Microbiol., **70:**3246–3252.

32a. **Rui, Li, K. F. Reardon, and T. K. Wood.** Altering toluene ortho-monooxygenase of *Burkholderia cepacia* G4 for regiospecific hydroxylation of indole to form indigoid compounds: Appl. Microbiol. Biotechnol., in press.

33. **Ryoo, D., H. Shim, K. Canada, P. Barbieri, and T. K. Wood.** 2000. Aerobic degradation of tetrachloroethylene by toluene-*o*-xylene monooxygenase of *Pseudomonas stutzeri* OX1. Nat. Biotechnol. **18:**775–778.
34. **Sakamoto, T., J. M. Joern, A. Arisawa, and F. H. Arnold.** 2001. Laboratory evolution of toluene dioxygenase to accept 4-picoline as a substrate. Appl. Environ. Microbiol. **67:**3882–3887.
35. **Sambrook, J., E. F. Fritsch, and T. Maniatis.** 1989. Molecular cloning: a laboratory manual, 2nd ed. Cold Spring Harbor Laboratory Press, Cold Spring Harbor, N.Y.
36. **Sanger, F., S. Nicklen, and A. R. Coulson.** 1977. DNA sequencing with chain-terminating inhibitors. Proc. Natl. Acad. Sci. USA **74:**5463–5467.
37. **Schmid, A., J. S. Dordick, B. Hauer, A. Kiener, M. Wubbolts, and B. Witholt.** 2001. Industrial biocatalysis today and tomorrow. Nature **409:**258–268.
38. **Schwede, T., J. Kopp, N. Guex, and M. C. Peitsch.** 2003. SWISS-MODEL: an automated protein homology-modeling server. Nucleic Acids Res. **31:**3381–3385.
39. **Shim, H., D. Ryoo, P. Barbieri, and T. K. Wood.** 2001. Aerobic degradation of mixtures of tetrachloroethylene, trichloroethylene, dichloroethylenes, and vinyl chloride by toluene-*o*-xylene monooxygenase of *Pseudomonas stutzeri* OX1. Appl. Microbiol. Biotechnol. **56:**265–269.
40. **Studts, J. M., K. H. Mitchell, J. D. Pikus, K. McClay, R. J. Steffan, and B. G. Fox.** 2000. Optimized expression and purification of toluene 4-monooxygenase hydroxylase. Protein Expr. Purif. **20:**58–65.
41. **Sun, A. K., and T. K. Wood.** 1996. Trichloroethylene degradation and mineralization by pseudomonads and *Methylosinus trichosporium* OB3b. Appl. Microbiol. Biotechnol. **45:**248–256.
42. **Tao, Y., A. Fishman, W. E. Bentley, and T. K. Wood.** Oxidation of benzene to phenol, catechol, and 1,2,3-trihydroxybenzene by toluene 4-monooxygenase of *Pseudomonas mendocina* KR1 and toluene 3-monooxygenase of *Ralstonia pickettii* PKO1. Appl. Environ. Microbiol., in press.
43. **Whited, G. M., and D. T. Gibson.** 1991. Separation and partial characterization of the enzymes of the toluene-4-monooxygenase catabolic pathway in *Pseudomonas mendocina* KR1. J. Bacteriol. **173:**3017–3020.
44. **Xu, D., D. P. Ballou, and V. Massey.** 2001. Studies of the mechanism of phenol hydroxylase: mutants Tyr289Phe, Asp54Asn, and Arg281Met. Biochemistry **40:**12369–12378.